Elsevier Editorial System(tm) for
Microporous & Mesoporous Materials
Manuscript Draft

Manuscript Number: MICMAT-D-17-00532R1

Title: Thermal behavior of stilbite and stellerite revisited and dehydration of their Na-exchanged forms: considerations on the memory effect of the STI framework type

Article Type: Full length article

Keywords: stellerite, stilbite, STI-framework type, Na-stellerite, Na-stilbite

Corresponding Author: Dr. Georgia Cametti, Ph.D.

Corresponding Author's Institution: Bern University

First Author: Georgia Cametti, Ph.D.

Order of Authors: Georgia Cametti, Ph.D.; Martin Fisch, PhD; Thomas Armbruster, Professor

Abstract: The thermal behavior of Na-exchanged stellerite and stilbite was investigated by in-situ single crystal X-ray diffraction. For comparison with the exchanged forms new data were collected on natural stellerite and stilbite under the same experimental conditions. With the increase of temperature, strong disorder at T and O sites of the tetrahedra of the four-membered ring developed in natural forms. Such disorder was associated with the rupture of T-O-T connections and transition from the A to the B phase. Differently from previous studies, stellerite B at T >300°C was found to be monoclinic (space group A2/m). In addition, at 400°C, a new T-O-T connection occurred, analogous to that in the B phase of barrerite.
Na-stellerite and Na-stilbite were at RT monoclinic, space group F2/m. Upon heating, they also displayed the same structural modifications as observed in natural barrerite and Na-barrerite and adopted space group A2/m. Compared to natural stellerite and stilbite different T-O-T connections ruptured leading to a different topology of the B phase. The total volume contraction was -16% at 350°C compared to -8% of pristine materials. The highly-condensed D phase, which does not form in natural stellerite and stilbite, was obtained by heating a Na-stellerite crystal ex-situ at 525°C. The structure corresponded to the D phase of natural barrerite and Na-barrerite.
All investigated STI members, after being exchanged with Na, have identical symmetry and demonstrate corresponding behavior upon heating and associated dehydration. Thus, a previously assumed memory effect of the symmetry of the natural parent structure, is not confirmed.

Cover letter

The present study reports a re-investigation of the dehydration process of natural stilbite and stellerite. Further, we produced Na-exchanged forms of these minerals and tracked their thermal behavior. The experiments were performed by *in-situ* single crystal X-ray diffraction.

We report differences with respect to previous studies and compare the structural behavior of natural and Na-forms upon heating. A final consideration is drawn about the memory effects of **STI** members.

With the present letter, we declare that the manuscript has not been submitted to another journal and all authors agreed to its submission.

Reviewers' comments:

Reviewer #1: This work reports new crystal structure data about the heat-induced transformations of STI-framework zeolites (stellerite, stilbite and barrerite) in their natural and Na-exchanged forms. The new results are compared and discussed with respect to previous studies.
Overall the manuscript is well written, the experimental work is of high quality and the discussion is sound. However, I believe that the paper needs to be improved on the following issues before publication:

- Introduction: "To rule out the influence of the experimental conditions we also collected new data on the natural forms and reinvestigated their thermal behavior." This sentence can be misleading. The reported work does not aim to provide any evidence that the influence of experimental conditions can be ruled out. So, for the sake of better clarity, I suggest to rewrite the sentence e.g. "In order to compare results obtained using the same experimental conditions we also collected new data on the natural forms and reinvestigated their thermal behavior by single crystal X-ray diffraction on quasi-equilibrated samples.";

A: Changed according to reviewer's comment.

- Experimental section - Samples: the chemical composition of stilbite sample from Poona used in this study is taken as the one reported by Passaglia et al. 1978 (showing only Ca and Na as the EF cations). While this can be an acceptable approximation, it is strongly advisable to provide the actual chemical composition of the used stilbite crystals;

A: We replaced the chemical composition with the one estimated by SEM-EDS analyses performed on the same sample we used for the structural investigation. Lines 73-75 changed accordingly.

- Experimental section - SC-XRD: "exposed to a dry N2 atmosphere (RH = 0 %)." Which kind of trap is used to achieve "dry" N2? Studies by Bish and co-workers showed that common "dry" nitrogen contain H2O and a H2O trap is necessary to obtain "truly dry" N2.

A: We did not use any trap to obtain "truly dry" N2. Thus, the dry conditions mentioned in our study may not refer to a completely dry atmosphere, i.e. RH = 0%. However, we can state that the conditions under the current experimental set-up are almost zero or in any case are dry according to our previous experience on a scolecite sample (ref. Cametti et al. 2015 Microporous and Mesoporous Materials 208, 171-180). The difference between dry or almost dry does not influence the results, what matter is that this experimental conditions are referred as "dry" compared to experiments performed by inserting the crystal inside a capillary.
To make it clearer in the text we modified line 88-91 in: 'Under these experimental conditions, the sample was continuously exposed to an almost dry N_2 atmosphere and such set-up is referred as low P_{H2O} experiment. The N_2 producer ensures a H_2O content $\leq$ 5 ppm but N_2 is blown in an open system on the crystal possibly allowing minor contamination by environmental humidity.'

- Experimental section - SC-XRD: "…waiting time between the steps was 40 minutes." How the Authors made sure that the crystal was (quasi)equilibrated at the given temperature after 40 minutes and it was not still transforming during the 8-hours data collection?

A: We are pretty sure that the crystal was (quasi)equilibrated, i.e. it was not undergoing significant structural modifications during the data collection because in case it happened it would have been recognizable (Rint value of the merged reflections). Of course, during the data collection is not excluded that the structure can re-arrange itself but such changes are not appreciable.

- Experimental section - SC-XRD: "Pseudomerohedral twinning … was observed…" The twinning model was included in the SHELX refinements? If so, there were any changes (e.g. BASF) observed as a function of T?

A: Yes, it was and no significant changes were observed as a function of temperature. To make it clear we added in Table 1a,b and Table 2a,b also the BASF value obtained from SHelX twin

refinement. We also added the sentence "The fractional volume contribution of the twin components, expressed by BASF parameter according to SHELXL-2014 [27], is reported in Table 1a,b and 2a,b." in the experimental section 2.2.

- Experimental section - XRPD: "Due to pseudo-orthorhombic symmetry associated with pseudomerohedral twinning [100 010 00-1] of all the monoclinic structures, single-crystal measurements are not suitable to resolve the correct <beta> angle." The Authors might wish to point out that while the monoclinic check by XRPD was performed on crystals at RT, the attribution to monoclinic or orthorhombic symmetry of high-T structures is based only on SC-XRD;

A: Actually, the XRPD measurement was not aimed at a monoclinic check. As we stated in lines 93-100 all the structures (At RT and at HT) were checked by test refinements performed in orthorhombic and monoclinic symmetry. The XRPD data collection was aimed only at determining the true beta angle. To make it clearer we specified "at RT" at the beginning of section 2.3.

- Results - Natural samples - Stellerite: The reported symmetry change of stellerite B-phase from Amma to A2/m is intriguing. Do the Authors have an interpretation on what is causing the monoclinic distortion? The T-O-T bond breaking? The Ca atoms diffusion? Alternatively, have the Authors considered the possibility of an apparent change in symmetry caused by the temperature-induced variation of monoclinic pseudomerohedral twin domains (extent and orientation)?

A: We give a general interpretation in the 4.1 section at lines 287-290 "The reason is that EF cations in the fully hydrated state of the A phase are coordinated by H2O molecules and have no or only weak bonds to framework O. With increasing temperature and associated dehydration EF cations disorder and develop bonds to framework O. Thus, with increasing dehydration distortive electrostatic potentials act on the framework.''

It is also related of course to Ca diffusion as we reported in lines 354-360.

Concerning the change of twin domain, the change is from Amma to A2/m that is from an untwinned structure to a monoclinic twinned one. In any case, the change in twin contribution was not observed in our tests refinements performed in A2/m at lower temperature (lower than 300°C).

- Results - Natural samples - Stilbite: The Authors do not mention any relationship between the migration of Ca (and/or Na) atoms after removal of coordinated water molecules and the occurrence of T-O-T ruptures. As it was previously suggested that the diffusion of EF cations (in particular, Ca ions) might be the cause of bond breaking, a comment is expected.

A: We actually mentioned and discussed it in the 4.2.1 section, lines 367-368 when we described the dehydration mechanism that is the same for both stellerite and stilbite. In particular we reported the following sentence: "Ca diffusion to new low occupied EF sites causing disorder of framework T and O sites within the four-membered ring units".

- Discussion - monoclinic character of STI framework: "… several test-refinements in both orthorhombic and monoclinic symmetry were done on the same data set." Were these tests performed only for RT structure or also for HT structures?

A: We performed test-refinements also at high temperature. To make it clearer we add at line 96: '' at each temperature".

- Discussion - differences to previous studies: I think there is an important factor which the Authors are neglecting while discussing their results, viz. the different Ca/Na ratio of STI-type zeolites and samples. As recalled by the Authors "The crystal symmetry, either orthorhombic or monoclinic, of STI group members is governed by the electrostatic repulsion between extraframework cations [Galli and Alberti 1975]". Monoclinic symmetry of natural stilbite at RT is caused by repulsion of Na pushing the Ca ions out of the mirror plane. This repulsion is not occurring in stellerite (no Na ions) while in barrerite is much weaker due to the lower charge of Na ions and their distribution over low occupancy sites. Both stellerite and barrerite keeps an orthorhombic unit cell. Therefore the

composition of EF cations (and the related Si/Al ratio of framework) is clearly playing a fundamental role in defining the symmetry variations of STI-type zeolites in their natural forms (i.e. in the presence of H2O). When considering the symmetry changes upon dehydration one might argue that the increasing Na content favor the monoclinic symmetry (according to the Authors' results the B-phase in both Na-exchanged stellerite and barrerite is A2/m while its symmetry is Amma-A2/m and Amma in their natural forms, respectively). However, when considering the B-phase symmetry of natural of stellerite, stilbite and barrerite the same Na-induced-obliquity effect no longer holds true (barrerite -B, the Na STI zeolite, is Amma!). Thus, the Na/Ca+Na) ratio is a factor controlling the symmetry of STI zeolites but it is not straightforward to model its effect on symmetry change upon dehydration. I believe that the Authors should include these considerations while discussing their results. When taking into account the Na/Ca+Na) ratio, the different nature of stilbite A-to-B phase transition (first order vs. second order reported here) and stilbite-B symmetry (Amma vs. A2/m reported here) observed by Cruciani et al. 1997 is not a matter of "interpretation" as stated by the Authors (lines 299-301: "The stilbite transformation from F2/m to A2/m instead of Amma was proposed by Drebushchak et al. [19]. According to these authors, the structural changes in stilbite were gradual and described by a second-order phase transition. Our results are in agreement with this interpretation [19]."). Instead, one should consider that both the sample from Poona used in the present study (Na/Ca+Na=0.19) and the one used by Drebushchak et al. (Na/Ca+Na=0.22) have significantly less Na content than the sample used by Cruciani et al. (Na/Ca+Na=0.36). The Si/Al ranges from 3.0 (the formers) to 3.2 (the latter). A likely interpretation is that the lower Na/Ca+Na of both samples used in the present work and by Drebushchak et al. makes stilbite-B to adopt a stable "stellerite-like" monoclinic symmetry while the higher Na/Ca+Na of sample used by Cruciani et al. makes stilbite-B to behave more "barrerite-like" adopting the Amma symmetry.

A: On this point, we partially agree with the reviewer.

It is not completely true that it behaves more “barrerite –like”. It is not only a matter of symmetry (monoclinic or orthorhombic), in this case is a matter of structural transformations that in stilbite (this study and Cruciani) are completely different from those occurring in barrerite (B phases and dehydration mechanism are not equivalent). Thus, it is not a direct consequence of Na/(Ca+Na) ratio. We report in the following paragraph our explanation. The same paragraph has been added in the text at the end of section 4.1.
A new figure (figure S2) has been added as supplementary material.

‘’With the increase of temperature stilbite and stellerite are both monoclinic because of the strongly disordered Ca distribution. The electrostatic Ca potentials interact differently on the framework. In natural barrerite (the Na-rich member of **STI** group) there is only a low concentration of Ca, hence the corresponding monoclinic distortion does not occur (the B phase of barrerite stays orthorhombic) (Figure 4). At first glance, this seems to be in contradiction with the Na-exchanged forms, which remain monoclinic upon dehydration. However, two aspects must be considered:
(1) The cation distribution: At RT the cation distribution influences both the geometry (orthorhombic versus monoclinic) and the centering (*A*- versus *F*-centering). In the Na-exchanged forms and in natural barrerite such a distribution is different because natural barrerite also contains small amounts of other cations such as K, Ca, and Mg, which favor different EF sites compared to Na (Fig. S2). In contrast, if only Na is present in the Na-exchanged forms, the EF cations are distributed at similar atomic positions as occupied by Ca and Na in natural stilbite. Therefore, both have the common space-group symmetry *F*2/*m*. It is rather difficult to unequivocally determine the complex cation distribution in natural barrerite (due to similar scattering power of O and Na), but it is evident that the siting of EF cations has a different bearing on the framework if comparing the RT structures of barrerite, stilbite, and Na-barrerite (Fig. S2). The framework of orthorhombic barrerite is differently distorted compared to the one of the monoclinic Na-barrerite (and, as a consequence, to all the Na-exchanged **STI** forms).

(2) The cation content: If the only EF cation is Na, it provokes upon dehydration the same structural transformations, in terms of T-O-T rupture and B phase topology, as in natural barrerite with minor K, Ca, and Mg, although described in the monoclinic symmetry. In contrast, if Ca is the main EF cation, the EF cation interaction with the framework is strengthened and a different B phase is produced.

Thus, not only the symmetry (*A*2/*m* or *Amma*) but also the framework modifications at elevated temperature have to be accounted when describing the different B-phases. Even if the B-phases of the Na-stellerite and Na-stilbite are described in *A*2/*m* symmetry as those of natural stellerite and stilbite, it does not mean that they approach the same topology due to different T-O-T ruptures and formation of new framework connections.''

- Discussion - differences to previous studies: lines 336-337 "Our general interpretation of the dehydration mechanism is consistent for both stellerite and stilbite and can be summarized as follows:". I believe that the Authors should make more clear that their interpretation is only valid under the same experimental conditions adopted in the present study and with the chemical composition of their stilbite sample. Therefore, I recommend to rewrite this sentence, e.g. "Our general interpretation of the dehydration mechanism acting under the experimental conditions of this study (single crystal diffraction from quasi-equilibrated crystals, nominally dry atmosphere) is consistent for both stellerite and the Na-poor stilbite used in this study. It can be summarized as follows:".

A: We changed it according to Reviewer's comments but we rewrote it slightly different from what proposed by the Reviewer:
''Our general interpretation of the dehydration mechanism acting under the experimental conditions of this study (single crystal diffraction from quasi-equilibrated crystals, nominally dry atmosphere) is consistent for both stellerite and the stilbite. It can be summarized as follows:'.

Reviewer #3: The paper studied the thermal behavior of Na-exchanged stellerite and stilbite and the structure changement during the heating processes. The authors should compare and give the reasons of structural differences between in-situ and ex-situ heating to natural stellerite and stilbite, and the effects of Na+ to the structural changement. The authors should also supply the conclusions of the whole manuscirpt.

A: An additional discussion about the difference between the ex situ structure refinement by Alberti et al. (1978) and our in situ data has been added in the discussion section of the text, headed by the subtitle "*4.2.2 Differences between previous ex situ experiments and the current in situ measurements on natural stellerite"*

The detailed differences and explanation for the structural varieties based on the Na and Ca content, also requested by Reviewer (1) is now presented in lines 290-314 of the manuscript.

The paragraph *"4.3. The Na-exchanged forms and the memory effect in **STI** framework type"* actually represents the conclusions of the most relevant findings of the manuscript. However, we prefer the more specific subtitle shown above than the suggested term "Conclusions".

***Reviewer Suggestions**

Reviewers

1. Prof. Giuseppe Cruciani

DIPARTIMENTO DI FISICA E SCIENZE DELLA TERRA,
Università degli Studi di Ferrara
Via Saragat 1
44122 – Ferrara
giuseppe.cruciani@unife.it

2. Prof. Rossella Arletti

Dipartimento di Scienze della Terra,
Univeristà degli studi di Torino
Via Valperga Caluso, 35
10125- Torino

rossella.arletti@unito.it

3. Prof. Dr. G. D. Gatta
Dipartimento di Scienze della Terra,
Universita` degli Studi di Milano, Via Botticelli 23,
20133 Milan, Italy
e-mail: diego.gatta@unimi.it

Highlights

- B phase of natural stellerite changed from *Amma* to *A*2/*m* at 300°C
- B phase of natural stilbite remained monoclinic (s.g. *A*2/*m*)
- Strong disorder developed with the increase of T in both B stellerite and B stilbite
- Na-stilbite and Na-stellerite structure at RT was the same as Na-barrerite
- All Na-forms of **STI** group behave identically upon heating

*Graphical Abstract

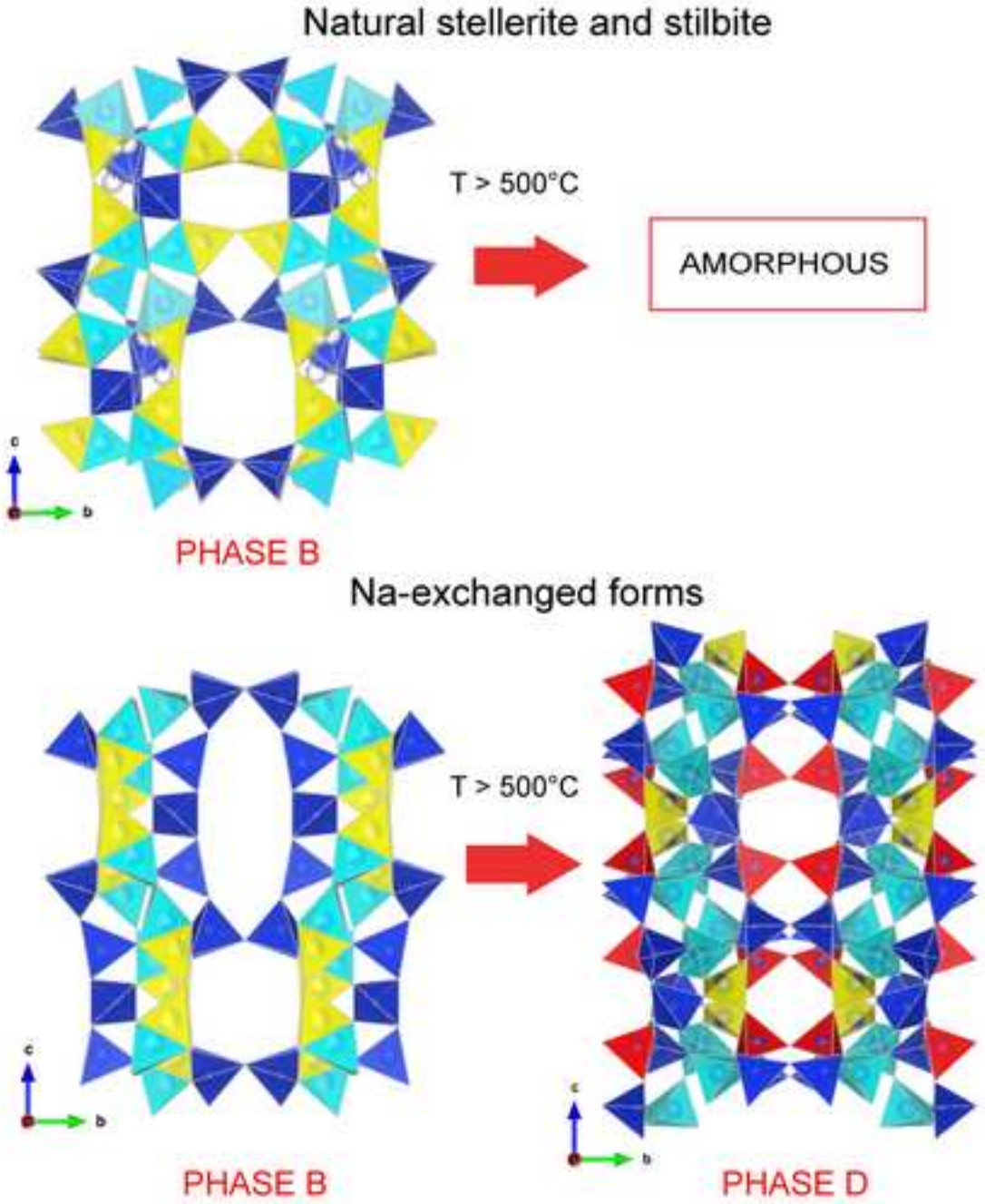

Thermal behavior of stilbite and stellerite revisited and dehydration of their Na-exchanged forms: considerations on the memory effect of the STI framework type

Georgia Cametti*[a], Martin Fisch[a], Thomas Armbruster[a]

[a]*Mineralogical Crystallography, Institute of Geological Sciences, University of Bern, Baltzerstr. 1+3, 3012 Bern, Switzerland*

Abstract

The thermal behavior of Na-exchanged stellerite and stilbite was investigated by *in-situ* single crystal X-ray diffraction. For comparison with the exchanged forms new data were collected on natural stellerite and stilbite under the same experimental conditions. With the increase of temperature, strong disorder at T and O sites of the tetrahedra of the four-membered ring developed in natural forms. Such disorder was associated with the rupture of T-O-T connections and transition from the A to the B phase. Differently from previous studies, stellerite B at T >300°C was found to be monoclinic (space group *A*2/*m*). In addition, at 400°C, a new T-O-T connection occurred, analogous to that in the B phase of barrerite.

Na-stellerite and Na-stilbite were at RT monoclinic, space group *F*2/*m*. Upon heating, they also displayed the same structural modifications as observed in natural barrerite and Na-barrerite and adopted space group *A*2/*m*. Compared to natural stellerite and stilbite different T-O-T connections ruptured leading to a different topology of the B phase. The total volume contraction was -16% at 350°C compared to -8% of pristine materials. The highly-condensed D phase, which does not form in natural stellerite and stilbite, was obtained by heating a Na-stellerite crystal *ex-situ* at 525°C. The structure corresponded to the D phase of natural barrerite and Na-barrerite.

All investigated **STI** members, after being exchanged with Na, have identical symmetry and demonstrate corresponding behavior upon heating and associated dehydration. Thus, a previously assumed memory effect of the symmetry of the natural parent structure, is not confirmed.

Keywords: stellerite, stilbite, STI-framework type, Na-stellerite, Na-stilbite

1. Introduction

Stilbite $Na_2Ca_8Al_{18}Si_{54}O_{144}\cdot 60H_2O$, and stellerite $Ca_8Al_{16}Si_{56}O_{144}\cdot 58H_2O$ are, together with barrerite $Na_{16}Al_{16}Si_{56}O_{144}\cdot 52H_2O$, natural zeolites belonging to the **STI** framework type. In nature barrerite does not occur as Na end-member but has a more complex composition and represents the Na-dominant species. The structure topology of the **STI** framework-type has *Fmmm* symmetry and consists of two sets of interconnected channels: one parallel to [100], confined by a ten-membered ring, and the other one running parallel to [001] confined by an eight-membered ring [1]. The structural difference between minerals in this group is based on symmetry controlled by the extraframework (EF) cations and their distribution within the zeolitic channels. The highest symmetry of the room-temperature (RT) phases, the so called A phases, is *Fmmm*, which is the space group of stellerite [2-4]. Barrerite is also orthorhombic but with the lower space-group symmetry *Amma* [5,6], whereas stilbite is monoclinic *C*2/*m* [7] and usually described in the pseudo-orthorhombic setting *F*2/*m* [8-11].

These zeolites are characterized by largely disordered Si/Al distributions [11-14] but local Si/Al order was proposed for stilbite, explaining deviations from monoclinic symmetry [15]. The same authors suggested growth sectors of different symmetry in stilbite crystals.

The dehydration behavior of members of the **STI** framework-type has been thoroughly investigated by X-ray diffraction techniques [3,4,10,16-19]. The structural modifications occurring with the increase of temperature involve the statistical breaking of T-O-T linkages and the formation of a new phase, the B phase of space group *Amma*. It is characterized by statistically occupied face-sharing tetrahedra associated with volume contractions of ca. -8% for stellerite and stilbite [4,10] and -16% for barrerite [18] with respect to the A phase at room temperature. Stilbite transforms to the B phase at 170°C [10], barrerite at 250°C [18] and, stellerite at ca. 160°C [4]. Although the A phases transform to the B phases accompanied by breaking of T-O-T connections, ruptured and newly formed T-O-T units differ topologically in stellerite and stilbite from those in barrerite.

Interestingly, *ex-situ* experiments performed on a single crystal of stellerite [3] resulted also in a similar type of B-phase found for barrerite. This disagreement has been interpreted as being related to the different experimental conditions, e.g. *in-situ* synchrotron X-ray powder diffraction [4] and single crystal X-ray diffraction on an *ex-situ* heated sample [3]. However, different experimental set-ups [16,18,20] do not influence the behavior of barrerite, which is always characterized by the breaking of the same T-O-T links.

T-OH terminations in the B phases were also suggested [4,16,21,22], though such terminations were more evident in the stellerite and stilbite structures than in the one of barrerite [4,10,16,22]. An additional transformation to a highly-condensed D phase (volume contraction of ca. -20% compared to the RT value) occurs only in barrerite at ca. 400-450°C [17]. Instead, stilbite and stellerite turn amorphous with increase of temperature.

Recently, we investigated the dehydration behavior of a natural sample of barrerite $Na_{8.24}K_{3.04}Ca_{2.24}Mg_{0.24}Al_{16.8}Si_{54.96}O_{144}\cdot 50H_2O$ fully exchanged with Na [20]. We found that the Na-barrerite structure at room temperature is monoclinic *F*2/*m* (same space group as for stilbite). Although the dehydration proceeds via a similar volume trend as observed for the natural barrerite, at 50°C the Na-exchanged structure changes from *F*2/*m* to *A*2/*m* (both space groups in pseudo-orthorhombic setting). In contrast to the "memory effect" proposed by Passaglia et al. [23], i.e. the capacity of the **STI** members "to remember" the original framework symmetry after exchanging their EF cations, we suggested that all Na-exchanged forms of the members of the **STI** framework-type are symmetrically identical and the structure does not maintain its original symmetry.

In this paper, we aim to test this assumption by extending the study to Na-exchanged stellerite and stilbite under the same experimental set-up used before for the Na-exchanged barrerite [20]. In order to compare results obtained using the same experimental conditions we also collected new data on the natural forms and reinvestigated their thermal behavior by single crystal X-ray diffraction on quasi-equilibrated samples.

2. Experimental section

2.1. Samples and cation exchange

The stellerite sample used in the present study originates from Gibelsbach, Fiesch (Valais, Switzerland, same sample used in Armbruster et al. [24]) whereas the stilbite crystals are from Poona District, India. The chemical compositions of the investigated samples are $Ca_{7.89}Na_{1.86}(Si_{53.91}Al_{18.25})O_{144}\cdot 63.60H_2O$ for stilbite (determined

from EDS-SEM analyses on 5 analytical points, water content according to structural refinement) and $Ca_{7.96}K_{0.83}Na_{0.33}(Si_{55.4}Al_{16.42})O_{144}\cdot 58.24H_2O$ for stellerite [24].

Crystals with dimensions ranging from 0.2 to 1 mm were placed in a Teflon autoclave filled with 2 M NaCl solution for 4 weeks at 100(5)°C. The NaCl solution was renewed every three days. In the case of stilbite it was necessary to prolong the exchange time to 8 weeks because a preliminary check indicated that the crystals were not completely exchanged. After the exchange process, the crystals were washed with deionized water and chemically examined by energy dispersive spectrometry (EDS) using a scanning electron microscope.

2.2. Single crystal X-ray diffraction (SC-XRD)

X-ray diffraction data were collected using a BRUKER APEX II single crystal X-ray diffractometer with Mo*K*α radiation (λ = 0.71073 Å) and a CCD area detector. In all experiments, the analyzed crystal was glued onto the tip of a glass fiber. The dehydration process was investigated in steps of 25 °C by using a self-constructed temperature controlled N_2-blower. Under these experimental conditions, the sample was continuously exposed to an almost dry N_2 atmosphere and such set-up is referred as low P_{H2O} experiment. The N_2 producer ensures a H_2O content ≤ 5 ppm but N_2 is blown in an open system on the crystal possibly allowing minor contamination by environmental humidity. Each data collection lasted ca. 8 h and the waiting time between the steps was 40 minutes. Crystal data and refinements parameters of each measurement are summarized in Tables 1a,b and 2a,b.

The data were integrated and an empirical absorption correction was applied using the Apex 2v. 2011.4-1 software package. Structures were solved using Shelxtl-2008 [25]. Structural refinements were carried out by SHELXL-2014 [26] using neutral atomic scattering factors. Before assigning either the monoclinic or orthorhombic symmetry, test refinements were performed in both crystal systems at each temperature. In general, our arguments in favor of the monoclinic symmetry over the orthorhombic one are based on:

1) Internal agreement factors (R_{int} ad R_{sigma}) of symmetry equivalent reflections;

2) Weighting scheme;

3) Final R value of the structural refinements.

All the monoclinic structures were solved in the space group *C*2/*m* but at RT the non-standard setting *F*2/*m* [10,27] was preferred for easy comparison with the orthorhombic structures. The pseudo-orthorhombic setting *A*2/*m* was chosen for monoclinic structures at higher temperatures (see next paragraph) to maintain the same axial orientation as for space group *F*2/*m* [20]. Pseudomerohedral twinning (matrix [100 010 00-1]) was observed for all data sets refined in the monoclinic space groups. The fractional volume contribution of the twin components, expressed by BASF parameter according to SHELXL-2014 [26], is reported in Table 1a,b and 2a,b. Cif files of the refined structures have been submitted as supplementary materials.

Structure solution and refinement details of natural samples

The structure of natural stellerite at room temperature was solved in space group *Cmmm* (transformed to *Fmmm*). Atomic coordinates and labels of framework sites were chosen as in [2]. Positions of extraframework cations and H_2O were determined by exploring difference Fourier maps. Structure solutions from 75 to 275°C indicated space group *Cmcm*, transformed to *Amma* [3,4]. For a better comparison, atomic coordinates and labels were those of barrerite in our previous study [20]. Thus, labels of atomic sites do not correspond to those used in

Ref. [4]. From 300 to 400°C, the structures were solved and refined in the monoclinic space group *A*2/*m* [20]. From 425 to 475°C, reflections split and only unit-cell parameters were extracted.

Natural stilbite at RT was refined in space group *F*2/*m*. Atomic labels and coordinates corresponded to those of Ref. [10]. Extraframework occupants were located from difference Fourier maps. From 75°C on, the structures were refined in space group *A*2/*m*. Atomic labels for framework sites of monoclinic stellerite were used. At 375°C we stopped the experiment because the crystal detached from the glass fiber.

Structure solutions and refinement details of Na-exchanged samples

At room temperature the Na-stellerite structure was pseudo-orthorhombic and was refined in the monoclinic space group *F*2/*m*. Atomic coordinates and labels were those of Na-barrerite [20]. At 50°C, a change from *F* to *A* centering was observed similarly to Na-exchanged barrerite and up to 400°C the structures were refined in space group *A*2/*m*. Atomic labels of framework atoms were those of Na-barrerite [20].

The RT Na-stilbite structure was solved in *F*2/*m*. At 50°C, the change from *F* to *A* centering, as for Na-stellerite, was observed.

Ex-situ experiment

In order to check whether the Na-exchanged samples transform to the D phase, the same experimental procedure as reported for the D phase of Na-barrerite [20] was used. A Na-stellerite crystal was gradually heated (65°C/h) up to 525 °C *ex-situ*. The temperature was kept for 4 h and the crystal was subsequently cooled for ca. 2 hours. For X-ray data collection at room temperature the sample was exposed to air. The structure was refined in space group $A2_1ma$ [17].

2.3 X-ray powder diffraction (XRPD)

We collected powder diffraction patterns at RT on samples of natural stilbite and Na-stellerite to obtain a more reliable β angle. Due to pseudo-orthorhombic symmetry associated with pseudomerohedral twinning [100 010 00-1] of all the monoclinic structures, single-crystal measurements are not suitable to resolve the correct β angle. Stilbite crystals were selected from two different specimens from the Poona locality. The first (referred as stilbite1) was the same as used for the Na-exchange experiment: pink platy stilbite crystals (ca. 50 × 30 × 5 mm) intergrown to bow-tie like clusters on laumontite. The second (referred as stilbite2) consisted of intergrown white silky crystals (ca. 15 × 5 × 2 mm) associated with cavansite.

The samples were gently powdered in an agate mortar. Subsequently, the powder was transferred onto a flat zero-background silicon sample holder and measured with a PANalytical X'Pert Pro MPD diffractometer equipped with a Cu X-ray tube and an X'Celerator detector. Each sample was measured using an irradiated length of 10 mm from 8 to 70° 2θ (corresponding to a resolution of 1.35 Å), a step size of 0.0167°/step and an acquisition time of 120 s/step.

Diffraction patterns were Pawley refined using TOPAS Academic V6 [28] starting from lattice parameters of stilbite and Na-stellerite obtained from single crystal data (this study) in space group *C*2/*m* and *F*2/*m*. Sample displacement and background parameters were also refined.

3. Results

3.1 Natural samples

Stellerite

The atomic coordinates, occupancy and atomic displacement parameters of natural stellerite at RT are reported in Table S1. Those obtained at 125, 175, 300, 350 and, 400°C in Tables S2, S3, S4, S5 and, S6. At room temperature the stellerite structure was consistent with previous models [2,4]. However, based on electron density in difference Fourier maps, we positioned seven additional partially-occupied sites (interpreted as H_2O molecules) within the structural cages (Table S1). Moreover, a very low occupied (*occ.* = 0.013(4)) calcium site was detected 0.61(4) Å apart from Ca1. We attributed such variations to the different chemical composition of the sample used in the present study compared to that used by Galli and Alberti [2] and Arletti et al. [4].

The dehydration started at 50°C and at 75°C the structure changed from space group *Fmmm* (A phase) to *Amma* (B phase) accompanied by a decrease of the unit-cell volume from 4419.3(1) at RT to 4202.1(4) $Å^3$ and by narrowing of the ten-membered ring channels. At 125°C, the statistical breaking of the T1P-O3P-T4 bonds (corresponding to T1-O3-T4 in ref. [4]) began. T1P started migrating towards the new tetrahedral site T1PD (*occ.* = 0.050(2)) whereas corresponding diffusion of the T4 site to a new position was not detected at this temperature (Table S2).

At 175°C, additional dehydration accompanied by structural contraction (Fig. 2a,b) led to increase of the percentage of ruptured bonds (T1PD, *occ.* = 0.230(2)) and to the formation of the T1PD-OD-T1PD connection (Table S3). The new OD site with refined occupancy 0.230(2) was at the corresponding position of the W14 site occupied at RT by a H_2O molecule inside the 10-membered ring channel (Fig. 2b). The occupancy of the OD site converged without constraints to the same value as that of the T1PD site, meaning that it does represent a shared oxygen between the two new T1PD sites related by the mirror plane (010) at y = 0, ½. At this temperature, the appearance of new peaks in difference Fourier maps indicated disorder close to the O3P and T4 sites. In particular, a new site (T4A, *occ.* = 0.11(2)) was detected 0.5 Å apart from T4 and additional electron density arose at ca. 0.94 and 1.55 Å from O3P and T4, respectively. At this stage, this peak was assigned to oxygen due to splitting of the O3P site. This assumption was based on the unconstrained occupancies, of T4 (*occ.* = 0.82), T4A (*occ.* = 0.14), O3P (*occ.* = 0.90) and, O3PA (*occ.* = 0.15). The final structure refinement of stellerite B at 175°C, containing occupancy constraints is reported in Table S3.

With the increase of temperature, the B structure of stellerite gradually changed to monoclinic. Between 200 and 300°C test refinements were performed in both orthorhombic (space group *Amma*) and monoclinic (*A2/m*); in spite of the better agreement indices for the monoclinic refinements, the orthorhombic symmetry was maintained up to 275°C because correlations, due to pseudo-symmetry in the monoclinic model, did not allow to properly resolve the disorder.

Differently from previous studies [3,4], at 300°C the crystal structure of partially dehydrated stellerite was refined in the monoclinic space group *A*2/*m* (Table S4). The correspondence between the tetrahedral sites in the orthorhombic and monoclinic space group is reported in Table 3 and in fig.2b,c. The T1P-O3P-T4 linkage, in space group *Amma*, corresponds in *A*2/*m* to two connections related by pseudo-symmetry: T1-O3M-T4 and T2M-O5M-T4M. Thus, the disorder first detected in the orthorhombic structure at 175°C was reflected in the monoclinic one by corresponding peaks (O3MA, O3M1 and O5MA) close to the O3M and O5M sites (Table S4).

With the increase of temperature, O3M1, O3MA and O5MA sites start migrating further away from O3M and O5M sites (approaching positions closer to T sites) and, at 350°C they were refined instead of O with Si

scattering factors and their labels were changed accordingly; O3MA and O3M1 merged to T4MD and O5MA was changed into T4D (Table S5; Fig. 3a,b). Nevertheless, these sites should be considered as occupied by a mixture of Si/Al and O atoms. Additional peaks also appeared close to T2 and T1M sites (*occ*.< 1); however, in this data set, only one new site (T2A) could be located at 1.225(16) Å from T2. At 400°C, the unit-cell volume further contracted to 3997.0(3) $Å^3$ (ca. -10% of that measured at RT) and the disorder significantly increased as demonstrated by the necessity of splitting additional oxygen sites (O3M, O8M and O1) (Table S6). Moreover, two additional sites, T1MA and T1MD, were detected close to T1M. Similarly to the barrerite B phase the new connection T4D-OD1-T2D formed inside the ten-membered ring channel (Fig. 2d). Final occupancies of the new T sites are reported in Table S6.

Stilbite

Structural data of stilbite at RT are reported in Table S7. Our results were in agreement with reference data [7,10]. As in stellerite, the main difference to previous refinements is the number of H_2O sites inside the channels. Due to the deficiency of X-ray single-crystal data to determine correct β angles from twinned pseudo-orthorhombic structures, unit-cell parameters refined from XRPD data at RT are presented in Table 4. The second stilbite specimen (stilbite2), although from the same locality, has a larger β angle (90.537(7)°) compared to stilbite1 (90.194(5)°).

The dehydration behavior developed through a mechanism similar to that observed in stellerite. Also in this case the main transformations at 75°C consist of the change from *F* to *A* centering and statistical breaking of the T-O-T connection. In contrast to previous findings [10], stilbite remained monoclinic and, at 75°C, transformed from space group *F*2/*m* to *A*2/*m*. Despite the difference in the crystal system the structural transformations were the same as those reported in stellerite. At 125 °C, the statistical breaking of the two linkages T1-O3M-T4 and T2M-O5M-T4M, related by pseudo-symmetry, started (Table S8). The percentage of ruptured connections corresponded to the value observed in stellerite. This led to a system of face-sharing tetrahedra and to the occlusion of the 10-membered ring channel. The occupancy of the two new apices (OD and ODM) converged at 350°C to 0.391(12) (without constraints), as that of the new T sites T1D and T2MD (occ. = 0.396(2)) (Table S9). Thus, similarly to stellerite, the oxygen atoms between the new tetrahedra are not hydroxylated. T1D and T2MD are always connected by an oxygen to their symmetry equivalent sites (analogous to Fig. 2c). With increasing temperature, the stilbite B phase was also affected by the complicate disorder system observed in stellerite B. The broad electron density cloud close to the oxygen at O3M and O5M and to Si/Al at the T4 and T4M sites was modeled by applying the same strategy as used for stellerite. Final structural refinement details of stellerite at 350°C are reported in Table S9.

3.2 Na-exchanged samples

Na-stellerite and Na-stilbite at room temperature

SEM-EDS spectra (Fig. S1) indicated complete Na-exchange and total absence of Ca atoms in stellerite and stilbite fragments. At room temperature the structures of Na-stellerite and Na-stilbite corresponded to that of Na-barrerite (Tables S10a,b). In particular, the EF occupants, H_2O and Na atoms, were distributed at the same sites as those reported in Na-barrerite.

The lattice parameters of Na-stellerite obtained from XRPD are reported in Table 4. In contrast to natural stilbite, the difference between the beta-angle value estimated by the two methods (90.060(2)° by SC-XRD and 90.076(6)° by XRPD) is insignificant.

Structural changes upon heating

The Na-exchanged forms of stellerite and stilbite followed a similar dehydration path upon heating. The unit-cell volume trend (Fig. 1) and the associated release of water as a function of temperature were analogous to those observed during *in situ* dehydration of natural barrerite and Na-barrerite [20]. The total contraction of the unit cell-volume was ca. -15% of that at RT. At 50°C, the change from *F* to *A* lattice centering occurred for both Na-exchanged forms. Nevertheless, some differences to Na-barrerite were observed.

As at 150°C in Na-barrerite, low occupied sites close to T1M and T4 indicated the beginning of T-O-T breaking involving the two connections T1M-O3-T4M and T4-O5-T2 (Tables S11a,b). Differently from Na-barrerite, the migration of the original T (T1M, T4M, T2 and T4) sites to the new positions (T1MD, T4MD, T2D and T4D) did not start simultaneously. Although the refined population of T4M and T2 sites was < 1 (Tables S11a,b), the flipping of such sites was only observed at 275°C. At this temperature, the new bonds T1MD-OD2-T4MD and T4D-OD1-T2D formed.

The heating process gradually induced changes on the Na-stellerite and Na-stilbite framework that led to similar channel contraction as observed for barrerite and Na-barrerite [20]. The progressive formation of disordered face-sharing tetrahedra led to the same structural configuration of the B phase (Fig. 2e) of natural and Na-barrerite at 350°C [20]. The final occupancies of the new T sites converged at 350°C to 40% (T4D and T2D) and 60% (T1MD and T4MD) for Na-stellerite and to 43% (T4D and T2D) and 58% (T1MD and T4MD) for Na-stilbite, respectively (Tables S12a,b), compared to 0.33% (T4D and T2D) and 0.66% (T1MD and T4MD) determined for Na-barrerite. Therefore, the structural transformations as well as the dehydration path are different from those reported for the natural stellerite and stilbite.

The *ex-situ* experiment performed on Na-stellerite yielded the highly-condensed D phase reported for natural barrerite and Na-barrerite [17,20]. The total volume contraction was of -19% that measured at RT. The D phase is orthorhombic in space group $A2_1ma$ (Table S13) without face-sharing tetrahedra. This structure maintained 50% of original tetrahedra involved in the T-O-T rupture and 50% of the new ones [20]. The 10-membered ring channel became occluded (compared to the B phase) by the flipping of additional tetrahedra (Fig. 2f) and the structure lost its microporous properties.

4. Discussion

4.1. The monoclinic character of the STI framework

The crystal symmetry, either orthorhombic or monoclinic, of **STI** group members is governed by the electrostatic repulsion between extraframework cations [5]. A correlation between the monoclinic β angle and the monovalent cation content was demonstrated for stilbite in space group *F*2/*m* [29]: the higher the Na occupancy at the Na specific site, the higher the deviation of β from 90°. However, the estimation of the β angle

in the monoclinic forms by single-crystal X-ray diffraction is not straightforward due to the twinned character of the pseudo-orthorhombic structures. In this particular case X-ray powder diffraction is more sensitive. Moreover, even in stilbite samples from the same locality β can vary significantly (Table 4). One would expect that all the Na-exchanged forms should have the same obliquity (i.e. the same β angle), due to the same content of EF cations. However, this is not the case due to slightly different Si/Al distributions [15] and therefore different electrostatic potentials within the cages. Only a data-collection strategy assuring high-redundancy allowed us to determine the correct space group. Furthermore, several test-refinements in both orthorhombic and monoclinic symmetry were done on the same data set. The monoclinic space groups were confirmed by structural refinements because pseudo-symmetry related sites did not behave in the same way (see for example T4 and T4M sites in the B phases of natural stellerite and stilbite).

A summary of the symmetries of the various **STI** phases is reported in Figure 4. The B phases of stellerite, stilbite and of the Na-exchanged forms of stilbite, stellerite and barrerite have a tendency to enhance the monoclinic distortion at higher temperatures. The reason is that EF cations in the fully hydrated state of the A phase are coordinated by H_2O molecules and have no or only weak bonds to framework O. With increasing temperature and associated dehydration EF cations disorder and develop bonds to framework O. Thus, with increasing dehydration distortive electrostatic potentials act on the framework.

With the increase of temperature stilbite and stellerite are both monoclinic because of the strongly disordered Ca distribution. The electrostatic Ca potentials interact differently on the framework. In natural barrerite (the Na-rich member of **STI** group) there is only a low concentration of Ca, hence the corresponding monoclinic distortion does not occur (the B phase of barrerite stays orthorhombic) (Figure 4). At first glance, this seems to be in contradiction with the Na-exchanged forms, which remain monoclinic upon dehydration. However, two aspects must be considered:

(1) The cation distribution: At RT the cation distribution influences both the geometry (orthorhombic versus monoclinic) and the centering (*A*- versus *F*-centering). In the Na-exchanged forms and in natural barrerite such a distribution is different because natural barrerite also contains small amounts of other cations such as K, Ca, and Mg, which favor different EF sites compared to Na (Fig. S2). In contrast, if only Na is present in the Na-exchanged forms, the EF cations are distributed at similar atomic positions as occupied by Ca and Na in natural stilbite. Therefore, both have the common space-group symmetry *F*2/*m*. It is rather difficult to unequivocally determine the complex cation distribution in natural barrerite (due to similar scattering power of O and Na), but it is evident that the siting of EF cations has a different bearing on the framework if comparing the RT structures of barrerite, stilbite, and Na-barrerite (Fig. S2). The framework of orthorhombic barrerite is differently distorted compared to the one of the monoclinic Na-barrerite (and, as a consequence, to all the Na-exchanged **STI** forms).

(2) The cation content: If the only EF cation is Na, it provokes upon dehydration the same structural transformations, in terms of T-O-T rupture and B phase topology, as in natural barrerite with minor K, Ca, and Mg, although described in the monoclinic symmetry. In contrast, if Ca is the main EF cation, the EF cation interaction with the framework is strengthened and a different B phase is produced.

Thus, not only the symmetry (*A*2/*m* or *Amma*) but also the framework modifications at elevated temperature have to be accounted when describing the different B-phases. Even if the B-phases of the Na-stellerite and Na-stilbite are described in *A*2/*m* symmetry as those of natural stellerite and stilbite, it does not mean that they approach the same topology due to different T-O-T ruptures and formation of new framework connections.

4.2. Natural stellerite and stilbite

4.2.1 Differences to previous studies

The results obtained on natural stellerite and stilbite indicated that upon heating the two minerals behave similarly. In particular, the volume contraction up to 350°C (-8.6 % for both structures) and the framework modifications accompanying the dehydration process are the same (Fig. 1). Due T-O-T bond rupture leading to partial flipping of tetrahedra into the 10-membered rings of the B phases, the rings are sub-divided into two 4- and one 6-membered units. The extraframework cations (Ca in stellerite and Na and Ca in stilbite) are disordered among partially occupied sites approximately at the same positions in both B stellerite and B stilbite.

The stilbite transformation from *F*2/*m* to *A*2/*m* instead of *Amma* was proposed by Drebushchak et al. [19]. According to these authors, the structural changes in stilbite were gradual and described by a second-order phase transition. Our results are in agreement with this interpretation [19]. In the natural forms, such transformations are identified by the change from *F*- to *A*-centering. In barrerite, this change does not occur (Fig. 4) and the transition from the A to the B phase is gradual [20], obscuring the boundary between the A and B phase. The change from *F* to *A* occurs for stellerite and stilbite at 75°C but the T-O-T ruptures begin at 150°C. Thus, it remains unclear whether the A-B transitions correspond to the change in lattice centering or to the inset of T-O-T breaking. In our opinion, it should be set in correspondence of the change of the lattice centering because T-O-T rupture is a gradual process.

The gradual transitions from the A to the B phases of stellerite and stilbite in our quasi-equilibrated experiments are also visible in the development of unit-cell volumes with temperature (Fig. 1). In contrast, in fast *in-situ* synchrotron X-ray powder diffraction studies [4,10] the A-B transitions are rather abrupt and shifted to higher temperature. Compared to previous *in-situ* synchrotron powder diffraction studies [4,10], our results showed several differences. In the B phases of both stellerite [4] and stilbite [10], hydroxyl groups at the OD site were suggested because the refined occupancy was found twice of that at T1D (in our study T1PD in *Amma*). In contrast, in our refinements the occupancies of corresponding oxygen sites (OD and ODM in the monoclinic structure) were found to be equal to those of the new tetrahedral sites (T1PD in *Amma* and T1D and T2MD in *A*2/*m*). Thus, OD and ODM share two T sites. This finding is in agreement with our assumption [20] that, whenever the structural topology facilitates it, "dry" experimental conditions prevent the formation of T-OH terminations. On the other hand, rupture of the T1P-O3P-T4 connection causes only the flipping of the T1P site (T1 and T2M in the monoclinic structure). This indicates that for charge balance an OH group must form at O3P (monoclinic O3M and O5M). In the B phases of stellerite and stilbite, up to 350°C, the T4 site remains at the same position and for charge balance the O3P site has no alternative to hydroxylation. Interestingly, at 300°C, the unit-cell volume (Fig.1) further decreases; we speculate that this decrease is associated with the release of the OH groups and, as a consequence, to the formation of the new T4D-OD1-T2D connection (Fig. 2d).

Our structural refinements also indicate the appearance of new T sites that have not been reported before. The T1MD and T2D sites, although low occupied, indicate the rupture of an additional T-O-T connection, equivalent to that broken in barrerite B.

The new data demonstrate that a complicated disordered system develops with increase of temperature, which includes all the tetrahedra of the four membered-ring. Such a system emerges from the combination of two effects: (1) Ca atoms migrate to new low occupied sites and induce strain on framework O. (2) Additional T

sites (T4, T4M, T2 and, T1M) partially migrate to new positions due to dihydroxylation. As an example, CN4 is the most populated (*occ.* = 0.312(8)) Ca site in the B phase of stellerite at 350°C. This site is in bonding distance between 2.11 and 2.7 Å to O3M, O5M, O7, O7M and, O2 (Fig. 5). An inspection of the electron density in the neighborhood of these sites (Fig. 3c,d) indicates a broadened cloud covering a large volume; thus our model with split sites is only a first approximation of dislocated electrons mainly close to O3M, O5M, T4 and T4M sites.

Our general interpretation of the dehydration mechanism acting under the experimental conditions of this study (single crystal diffraction from quasi-equilibrated crystals, nominally dry atmosphere) is consistent for both stellerite and the stilbite. It can be summarized as follows: (1) Initial dehydration accompanied by channel deformation and partial rupture of T-O-T connections followed by formation of new T-O-T links (Fig. 6a,b). (2) Further rupture of additional T-O-T links where only one T site migrates to a new position and the terminated tetrahedral apex is charge balanced by an OH group (Fig. 6c). (3) Ca diffusion to new low occupied EF sites causing disorder of framework T and O sites within the four-membered ring units; (4) Dihydroxylation with the increase of temperature. T sites with terminated tetrahedral apices flip/migrate to new positions and newly created T-O-T connections occur (Fig. 6d); (5) With loss of OH groups, the structures become increasingly strained and disordered and finally turn X-ray amorphous.

4.2.2 Differences between previous ex-situ experiments and the current in-situ measurements on natural stellerite

Structural modifications upon dehydration of the **STI** framework type strongly depend on kinetic parameters influenced by the heating procedure (timing) and the mode how dehydration is accomplished. Alberti et al. [3] increased the temperature of stellerite gradually for 6 h up to 220° C and kept this temperature for 16 h while the sample was simultaneously exposed to vacuum of 10^{-2} Torr in a glass capillary. Subsequently, the capillary was sealed and single-crystal diffraction data were collected under ambient conditions. This way they achieved a unit-cell volume of the stellerite B phase of 3897 $Å^3$. This value is ca. 5% smaller (Fig. 1) than the volume we measured *in situ* for a stellerite crystal that was stepwise (25°C) heated to 225°C and kept at each step for ca. 9 h under "dry" nitrogen. Actually, a similar unit-cell volume was measured by us for the B phase of stellerite only at 425°C. Structural analysis of the stellerite B phase (space group *Amma*) obtained by the *ex-situ* experiment [3] resulted in T-O-T bond rupture leading to ca. 10% "faces-sharing" tetrahedra of the type T1P/T1PD and T4/T4D. Their [3] stellerite B phase strongly resembles the B phase analyzed for natural barrerite and is significantly different to the stellerite B phase obtained by us (this study) and the fast non-equilibrium synchrotron dehydration study [4]. Thus, the major difference of the modification of the stellerite B phase between our results and those of Alberti et al. [3] is most probably not due to the difference *in-situ* versus *ex-situ* but due to the different heating and dehydration protocol.

*4.3. The Na-exchanged forms and the memory effect in **STI** framework type*

The experiments performed on the Na-exchanged forms of stellerite and stilbite confirmed our assumption that all **STI** members, after being exchanged with the same cation, have identical symmetry. Although at RT it may be difficult to appreciate the deviation from orthorhombic symmetry, at high temperatures the monoclinic character is evident. The high-temperature experiments clearly demonstrated that the Na-exchanged **STI** members behave identically upon heating, confirming that they cannot "remember" their original symmetry.

With respect to the natural forms, not only the volume contraction is more pronounced (-8% in natural forms and ca. -16% in Na-exchanged ones) but also the structural transformations are different (topology of the B phase). The most evident effect is the transformation of Na-stellerite to the D phase which in natural stellerite does not occur.

Acknowledgments

We thank two anonymous reviewers for their helpful comments on the manuscript.

References

[1] Ch. Baerlocher, W.M. Meier, D. H. Olson, Atlas of zeolite framework types, Structure commission of the IZA, Elsevier, 5th ed. 2001, 302p.

[2] E. Galli, A. Alberti, *Bull. Soc. Fr. Mineral. Cr.* 98 (1975a) 11-18.

[3] A. Alberti, R. Rinaldi, G. Vezzalini, *Phys. Chem. Miner*. 2 (1978) 365-375.

[4] R. Arletti, E. Mazzucato, G. Vezzalini, *Am. Mineral*. 91 (2006) 628-634.

[5] E. Galli, A. Alberti, *Bull. Soc. Fr. Mineral. Cr.* 98 (1975) 331-340.

[6] M. Sacerdoti, A. Sani, G. Vezzalini, *Micropor. Mesopor. Mat.* 30 (1999) 103-109.

[7] E. Galli, G. Gottardi, *Miner. Petrogr. Acta* 12 (1966) 1-10.

[8] M. Slaughter, *Am. Mineral*. 55 (1970) 387-397.

[9] W. J. Mortier, *Am. Mineral.* 68 (1983) 414-419.

[10] G. Cruciani, G. Artioli, A. Gualtieri, K. Ståhl, J. C. Hanson, *Am. Mineral*. 82 (1997) 729-739.

[11] E. Galli, *Acta Cryst*. B27 (1971) 833-841.

[12] E. Lippmaa, M. Mägi, A. Samoson, M. Tarmark, G. Engelhardt, *J. Am. Chem. Soc*. 103 (1981) 4992-4996.

[13] A. Sani, C. Marichal, C. Forte, *Plinius*, 22 (1999) 344-345.

[14] A. Sani, L. Del Motte, C. Marichal, Z. Gabelica, C. Forte, *Eur. J. Mineral*. 13 (2001) 101-111.

[15] M. Akizuki, H. Konno, *Am. Mineral.* 70 (1985) 814-821.

[16] A. Alberti, G. Vezzalini, in: L. B. Sand, J. Mumpton (Eds.), *Natural Zeolites. Occurrence, Properties, Use*, Pergamon Press, New York, 1978, pp. 85-98.

[17] M. Sacerdoti, *Micropor. Mesopor. Mat.* 102 (2007) 299-303.

[18] S. Ori, E. Mazzucato, G. Vezzalini, *Am. Mineral*. 94 (2009) 64-73.

[19] V. A. Drebushchak, S. N. Dementiev, Yu. V. Seryotkin, *J. Therm. Anal. Calorim*. 107 (2012) 1293-1299.

[20] G.Cametti, T. Armbruster, M. Nagashima, *Micropor. Mesopor. Mat.* 236 (2016) 71-78.

[21] A. Alberti, F. Cariati, L. Erre, P. Piu, G. Vezzalini, *Phys. Chem. Minerals*, 9 (1983) 189-191.

[22] P. S. R. Prasad, K. S. Prasad, S. R. Murthy, *Am. Mineral.* 90 (2005) 1636-1640.

[23] E. Passaglia, M. Sacerdoti, *Bull. Mineral*. 105 (1982) 338-342.

[24] T. Armbruster, T.Kohler, T.Meisel, T. F. Nägler, M. A. Götzinger, H. A. Stalder, *Schweiz. Mineral. Petrogr. Mitt.* 76 (1996) 131-146.

[25] G. M. Sheldrick, *Acta Cryst.* A64 (2008) 112-122

[26] G. M. Sheldrick, *Acta Cryst.* C71 (2015) 3-8.

[27] S. Quartieri, G. Vezzalini, *Zeolites* 7 (1987) 163-170.

[28] A. A. Coelho, TOPAS Academic Version 6, Coelho Software, Brisbane, Australia, 2016.

[29] E. Passaglia, E. Galli, L. Leoni, G. Rossi, *Bull. Mineral*. 101 (1978) 368-375.

440
441
442
443
444
445
446

Figure(s)

Click here to download high resolution image

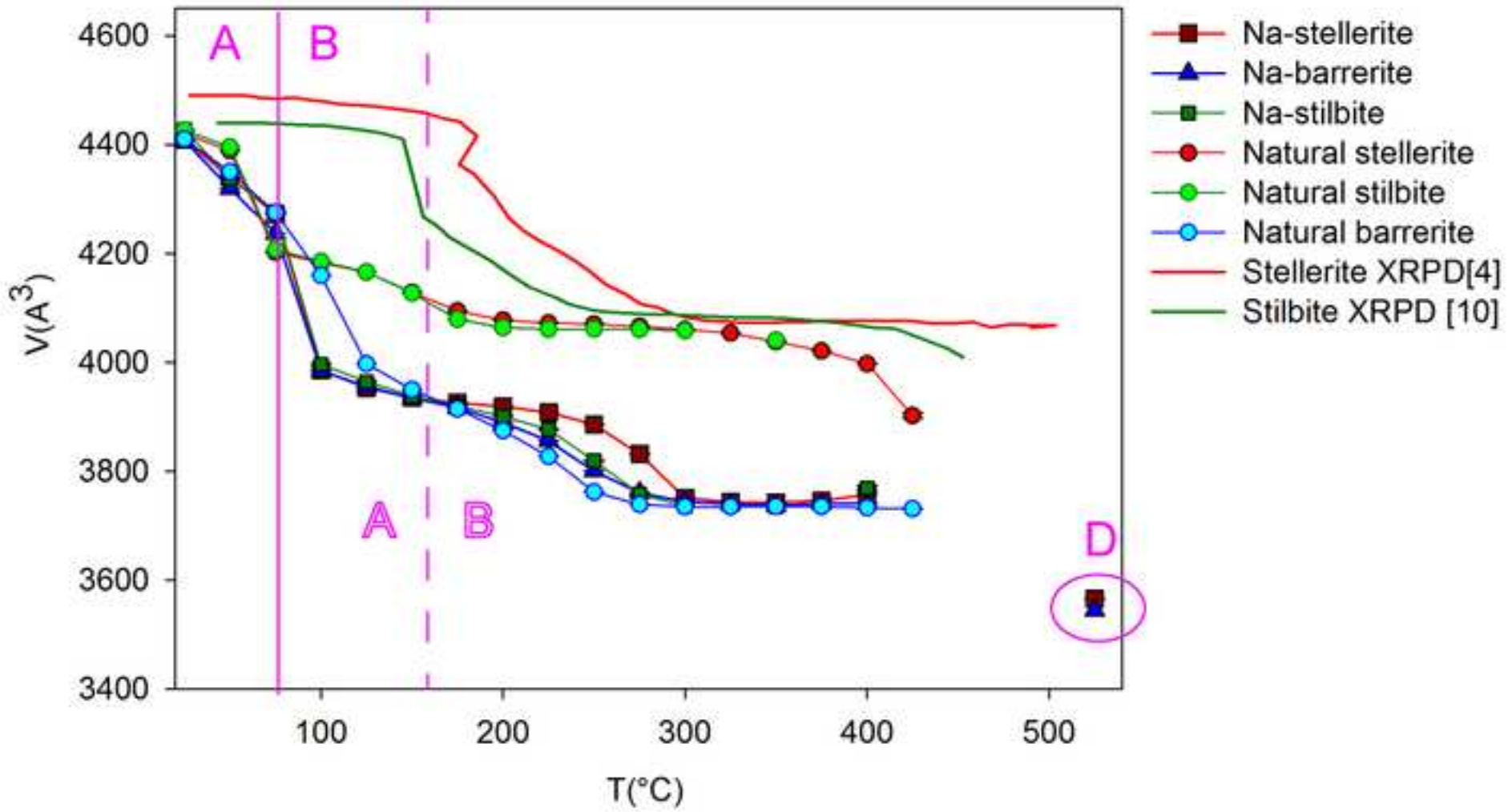

Figure2

Click here to download high resolution image

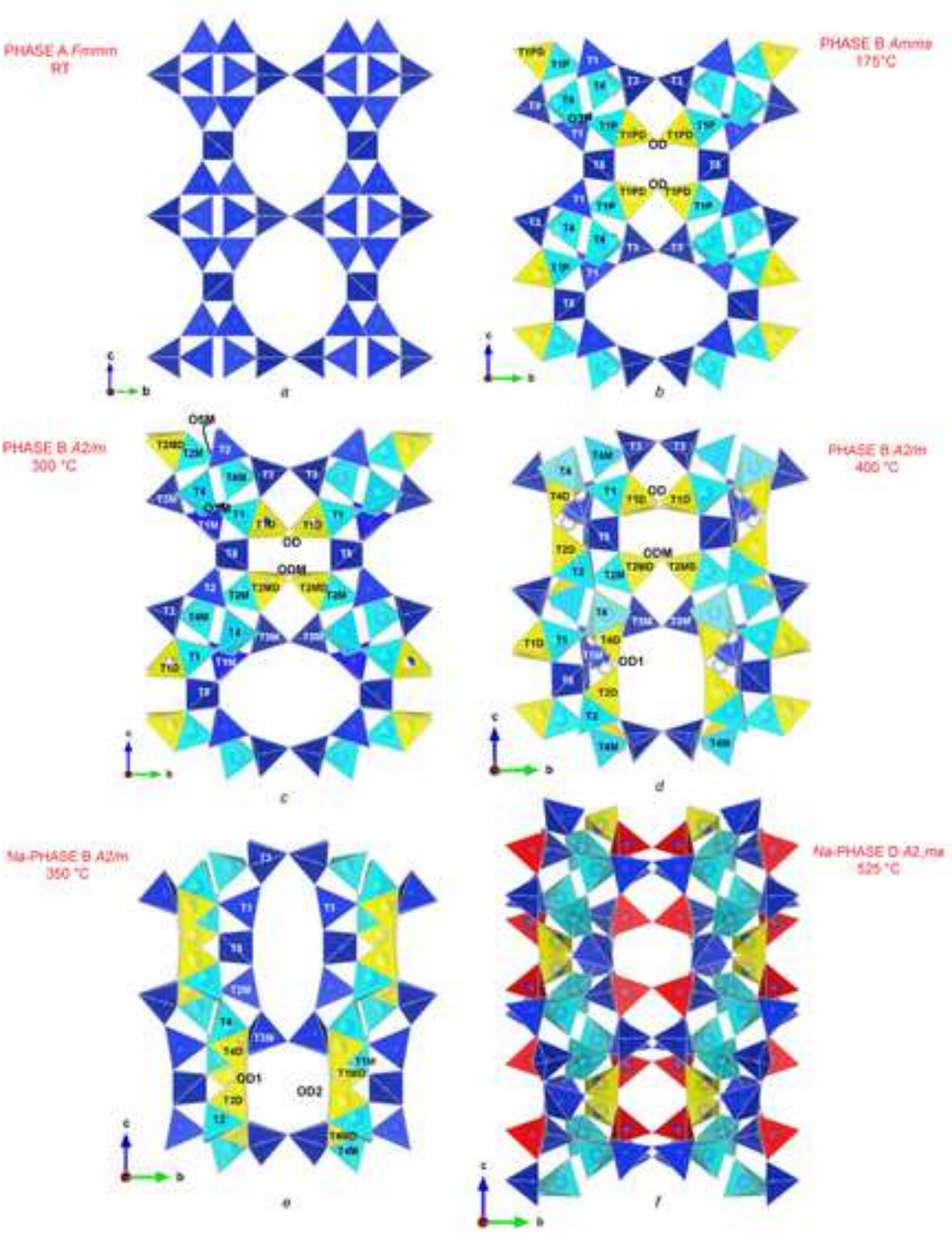

Figure3

Click here to download high resolution image

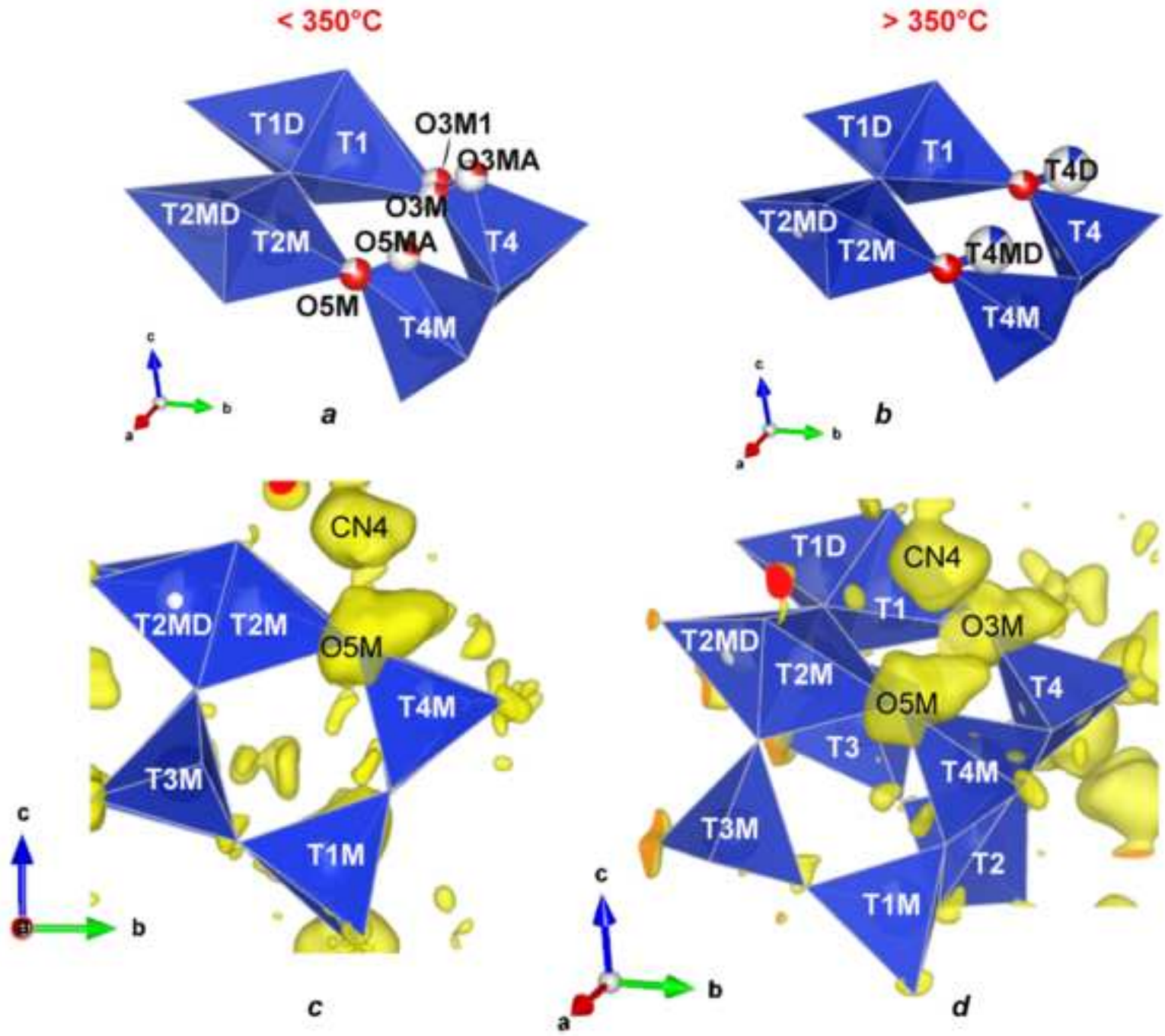

Figure4

Click here to download high resolution image

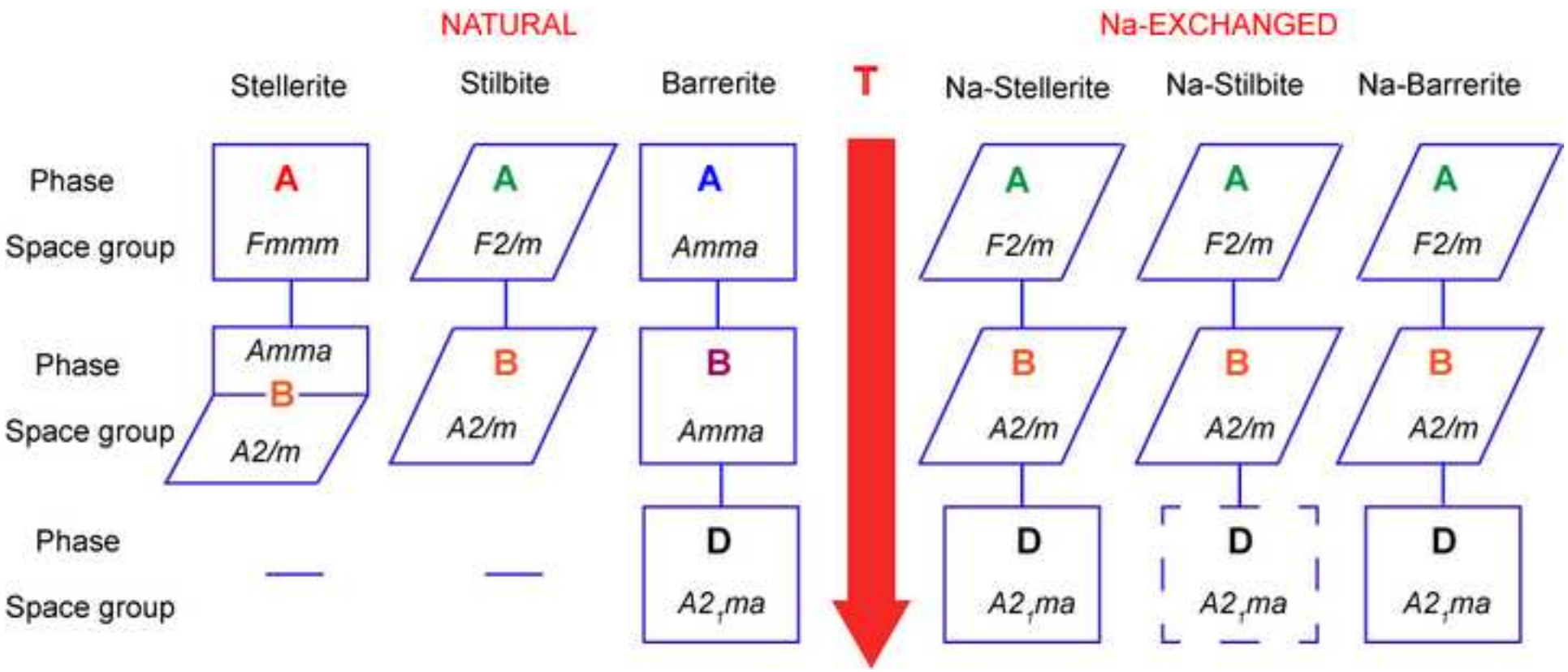

Figure5

Click here to download high resolution image

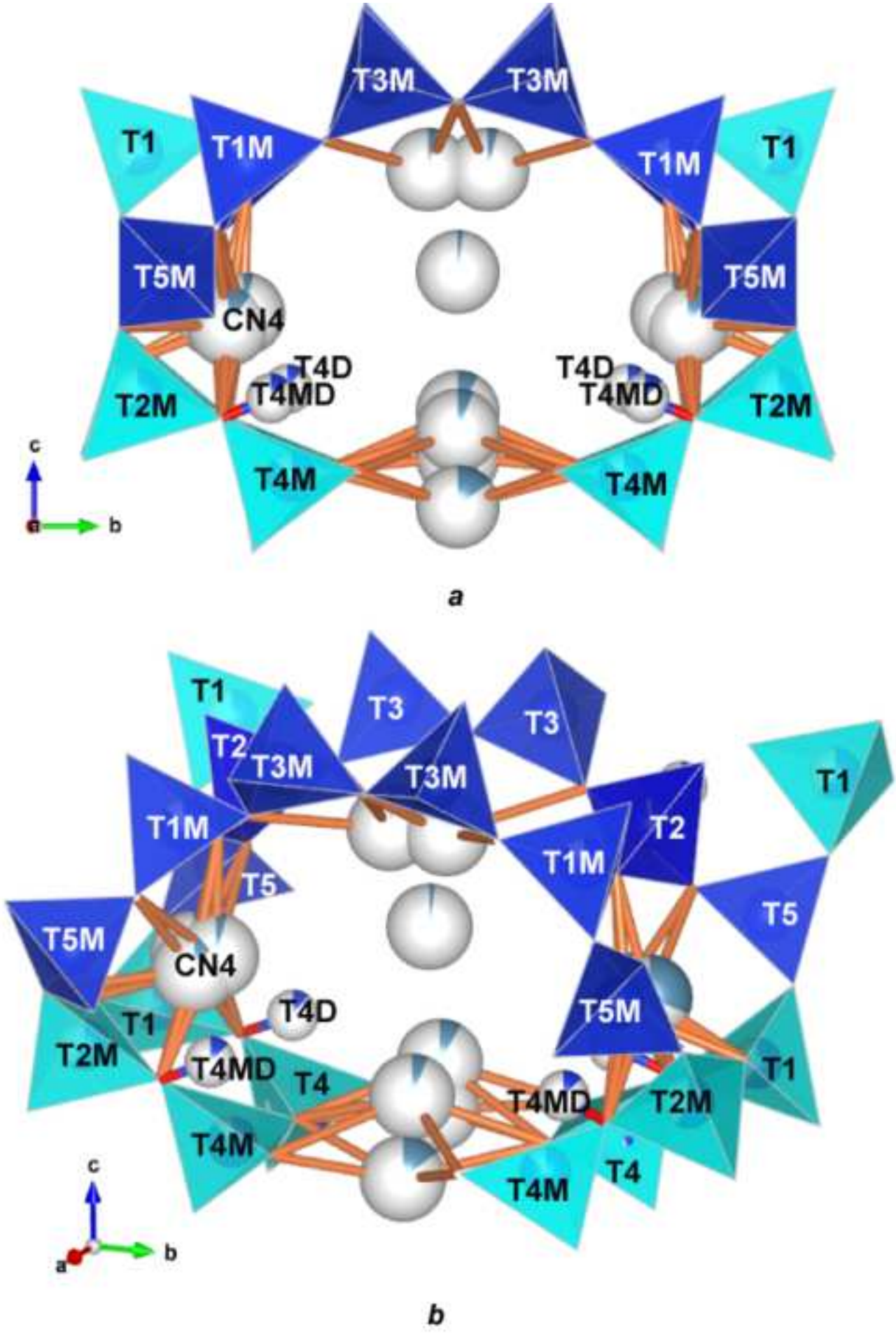

Figure6

Click here to download high resolution image

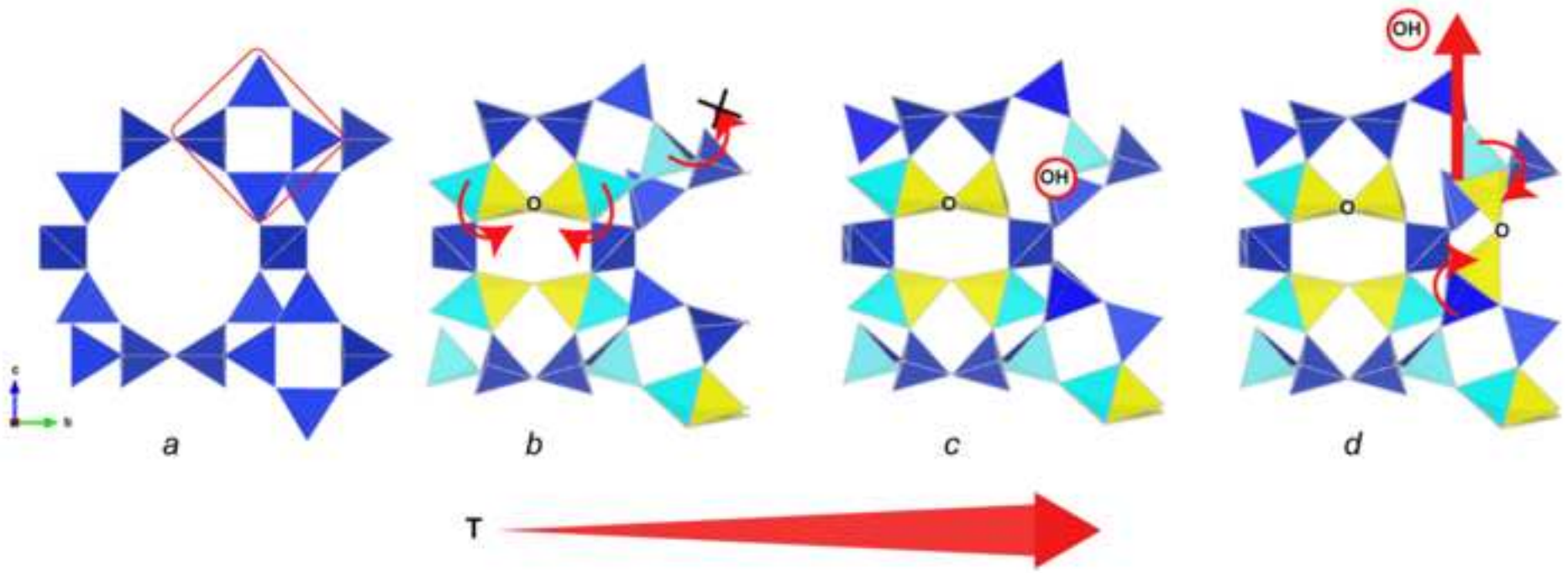

Figure captions

Figure 1 Unit-cell volume trend of natural and Na-exchanged forms of stellerite, stilbite, and barrerite [20] as a function of temperature. Synchrotron X-ray powder diffraction data (XRPD) are reported for comparison [4,10]. Unit-cell volumes of the D phase of Na-barrerite [20] and Na-stellerite (this study) obtained *ex-situ* in air are also shown. The vertical continuous line indicates the A-B transition temperature (set in correspondence of the change of lattice centering) for stilbite and stellerite as obtained in this study. The dashed line refers to the corresponding A-B transition reported in XRPD reference data.

Figure 2 Framework of the A phase of stellerite at RT (a) and of the B phase of stellerite at 175°C (b) and 300°C (c). $(Si,Al)O_4$ tetrahedra are depicted in blue. The original tetrahedra involved in the T-O-T rupture are shown in cyan whereas the new T sites originating as a consequence of the T migration are yellow. Sites are labeled to show the correspondence between the nomenclature of tetrahedra in orthorhombic and monoclinic symmetry. (d) Framework of the stellerite B phase at 400°C. The irregular shape of $(Si,Al)O_4$ tetrahedra is due to split oxygen sites. Partially colored spheres show low occupied T sites. (e) B phase of Na-exchanged forms of stellerite and stilbite at 350°C. (f) D phase of Na-stellerite obtained ex-situ in air. Red tetrahedra correspond to those flipped inside the cage.

Figure 3 Magnified view of the four-membered ring tetrahedra in the stellerite B phase at 350°C. The model is adopted to fit the electron cloud close to O and T sites up to 350°C (*a*) and from 350°C to 400°C (*b*). The occupancies of O and T sites are shown by partially colored red and blue spheres, respectively. (*c, d*) Calculated electron density in correspondence of O3M, O5M, T4D, T4MD and CN4 sites. Yellow isosurfaces correspond to electron density > 0.9 $e^-/Å^3$.

Figure 4 Diagram summarizing the space group of the A, B, and D phases for natural and Na-exchanged forms of **STI** members. The box around the Na-stilbite D phase is represented by a dashed line because it is assumed in correspondence to Na-stellerite.

Figure 5 Coordination of the Ca atoms in the stellerite structure at 350°C. (a) Detail of the stellerite cage parallel to the **a** axis. Cyan tetrahedra represent T sites involved in T-O-T rupture. Ca (CN4) and (Si,Al) atoms (T) are reported as partially colored light blue and blue spheres, respectively; Ca-O bonds are depicted as orange cylinders. (b) Same as (a) projected along a different direction to highlight the four-membered ring (T1,T2M,T4,T4M).

Figure 6 Schematic representation of the dehydration process of stilbite and stellerite. (a) Detail of the RT structure representing the ten- and four-membered ring (highlighted by the red rectangle). (b) Rupture of the T-O-T link (tetrahedra involved are colored in cyan), flipping of tetrahedra (indicated by the red arrows) and formation of the new T-O-T connection (in yellow) inside the ten-membered ring. Only one T site migrates and the other one is OH terminated (c). (d) Dihydroxylation as a consequence of the increasing temperature. Flipping of additional T sites and formation of new T-O-T connections.

Table(s)

Table 1a. Crystal data and refinement parameters of natural stellerite at RT, 125 (RH ~ 0), 175 (RH ~ 0), 300 (RH ~ 0), 350 (RH ~ 0) and 400°C (RH ~ 0).

Crystal data	**Stellerite A RT**	**Stellerite B 125°C**	**Stellerite B 175°C**	**Stellerite B 300°C**	**Stellerite B 350°C**	**Stellerite B 400°C**
Crystal size (μm)	150 x 200 x 100	150 x 200 x 100	150 x 200 x 100	150 x 200 x 100	150 x 200 x 100	150 x 200 x 100
a-axis (Å)	13.6132(2)	13.6877(8)	13.5964(4)	13.5488(2)	13.514(2)	13.5152(7)
b-axis (Å)	18.2106(2)	17.6156(10)	17.6163(5)	17.6133(3)	17.577(3)	17.5071(9)
c-axis (Å)	17.8266(2)	17.2760(10)	17.0929(4)	17.0125(2)	16.998(3)	16.8928(8)
β (°)	-	-	-	90.0125(2)	90.053(10)	90.028(3)
Cell volume ($Å^3$)	4419.30(10)	4165.5(4)	4094.06(19)	4059.85(10)	4037.7(12)	3997.0(3)
Z	1	1	1	1	1	1
Space group	*Fmmm*	*Amma*	*Amma*	*A*2/*m*	*A*2/*m*	*A*2/*m*
Refined chemical formula	$Ca_{7.54}(Si,Al)_{72}O_{144}\cdot 66.3H_2O$	$Ca_{7.29}(Si,Al)_{72}O_{144}\cdot 29.6H_2O$	$Ca_{7.16}(Si,Al)_{72}O_{144}\cdot 23.5H_2O$	$Ca_{7.81}(Si,Al)_{71.17}O_{144}\cdot 6H_2O$	$Ca_{7.80}(Si,Al)_{72.20}O_{142.95}$	$Ca_{6.90}(Si,Al)_{71.95}O_{145.5}$
Data collection						
Diffractometer			Bruker APEX II SMART			
X-ray radiation			Mo$K\alpha$ λ=0.71073 Å			
X-ray power			50 kV, 30 mA			
Monochromator			Graphite			
Temperature (°C)	25	125	175	300	350	400
Time per frame (s)	10	10	10	10	10	10
Max. 2θ	75.53	77.13	69.91	72.13	68.81	64.06
Index ranges	-21 < *h* < 23	-24 < *h* < 24	-21 < *h* < 21	-22 < *h* < 22	-21 < *h* < 21	-20 < *h* < 20
	-31 < k < 30	-30 < k < 30	-28 < k < 28	-29 < k < 28	-27 < k < 27	-26 < k < 25
	-30 < l < 30	-30 < l < 27	-25 < l < 27	-26 < l < 28	-26 < l < 25	-23 < l < 25
No. of measured reflections	39492	74100	60135	53347	48798	48085
No. of unique reflections	3207	6204	4762	9811	8662	7146
No. of observed reflections $I > 2\sigma(I)$	2740	4467	3522	5771	5319	4507
Structure refinement						
No. of parameters used in the refinement	132	242	270	382	367	355
R(int)	0.0364	0.0604	0.0697	0.0	0.0661	0.0762
R(σ)	0.0187	0.0303	0.0353	0.	0.0409	0.0475
GooF	1.078	1.039	1.038	1.006	1.013	1.034
*R*1, I>2$\sigma(I)$	0.0366	0.0459	0.0525	0.0527	0.0500	0.0559
*R*1, all data	0.0434	0.0679	0.0728	0.0991	0.0909	0.0949
w*R*2 (on F^2)	0.1109	0.1421	0.1612	0.1723	0.1618	0.1777
$\Delta\rho_{min}$ (-e$Å^{-3}$) close to	-0.53 W6	-0.68 Ca3	-0.64 T1	-0.54 T1M	-0.37 T3M	-0.57 O8
$\Delta\rho_{max}$ (e$Å^{-3}$) close to	0.82 W3	0.81 Ca6	0.73 O9	0.88 CN3	0.71 O6M	0.72 Ca3A
BASF				0.497(4)	0.505(4)	0.489(4)

Table 1b. Crystal data and refinement parameters of natural stilbite at RT, 125 (RH ~ 0) and 350°C (RH ~ 0).

Crystal data	**Stilbite1 A RT**	**Stilbite1 B 125°C**	**Stilbite1 B 350°C**
Crystal size (μm)	150 x 200 x 350	150 x 200 x 350	150 x 200 x 350
a-axis (Å)	13.6044(2)	13.6830(2)	13.542(3)
b-axis (Å)	18.2482(2)	17.6153(3)	17.581(4)
c-axis (Å)	17.8291(4)	17.2825(2)	16.986(4)
β (°)	90.0320(10)	90.0080(10)	90.165(13)
Cell volume (Å^3)	4426.18(13)	4165.60(11)	4044.1(15)
Z	1	1	1
Space group	*F*2/*m*	*A*2/*m*	*A*2/*m*
Refined chemical formula	$Ca_{7.94}Na_{2.60}(Si,Al)_{72}O_{144}\cdot 64.1H_2O$	$Ca_{6.36}Na_{1.69}(Si,Al)_{72}O_{144}\cdot 24H_2O$	$Ca_{6.40}Na_{1.76}(Si,Al)_{72.33}O_{143}$
Data collection			
Diffractometer		Bruker APEX II SMART	
X-ray radiation		Mo$K\alpha$ λ=0.71073 Å	
X-ray power		50 kV, 30 mA	
Monochromator		Graphite	
Temperature (°C)	25	125	350
Time per frame (s)	10	10	40
Max. 2θ	64.06	75.97	69.94
Index ranges	-20 < *h* < 20	-23 < *h* < 22	-20 < *h* < 21
	-27 < k < 27	-30 < k < 30	-26 < k < 38
	-25 < l < 26	-29 < l < 29	-27 < l < 23
No. of measured reflections	33374	47820	30522
No. of unique reflections	3889	11426	9058
No. of observed reflections $I > 2\sigma(I)$	3504	7296	5532
Structure refinement			
No. of parameters used in the refinement	210	365	341
R(int)	0.0263	0.0523	0.0487
R(σ)	0.0196	0.0449	0.0402
GooF	1.063	1.049	1.031
*R*1, I>2σ *(I)*	0.0327	0.0487	0.0550
*R*1, all data	0.0373	0.0843	0.0952
w*R*2 (on F^2)	0.0940	0.1541	0.1841
$\Delta\rho_{min}$ (-eÅ^{-3}) close to	-0.47 W12	-0.51 T5	-0.76 T4
$\Delta\rho_{max}$ (eÅ^{-3}) close to	0.53 W5	0.70 W6	0.69 O1M
BASF	0.396(4)	0.503(3)	0.498(4)

Table 2a Crystal data and refinement parameters of Na-stellerite at RT, 150 (RH ~ 0), 350 (RH ~ 0) and produced at 525°C (measured at RT).

Crystal data	**Na-stellerite A RT**	**Na-stellerite B 150°C**	**Na-stellerite B 350°C**	**Na-stellerite D 525°C**
Crystal size (μm)	150 x 200 x 500	150 x 200 x 500	150 x 200 x 500	150 x 100 x 100
a-axis (Å)	13.6195(2)	13.6539(3)	13.6031(4)	12.9893(15)
b-axis (Å)	18.1646(3)	17.1974(4)	17.1514(5)	16.872(2)
c-axis (Å)	17.8200(5)	16.7576(4)	16.0398(5)	16.2686(15)
β (°)	90.060(2)	90.0560(10)	90.061(2)	-
Cell volume (Å^3)	4408.54(16)	3934.88(16)	3742.28(19)	3565.4(7)
Z	1	1	1	1
Space group	*F*2/*m*	*A*2/*m*	*A*2/*m*	*A*2$_1$*ma*
Refined chemical formula	$Na_{18.85}(Si,Al)_{72}O_{144}{\cdot}50.6H_2O$	$Na_{14.60}(Si,Al)_{71.12}O_{144}{\cdot}6.9H_2O$	$Na_{13.79}(Si,Al)_{72}O_{144.1}$	$Na_{12.21}(Si,Al)_{72}O_{144}$
Data collection				
Diffractometer		Bruker APEX II SMART		
X-ray radiation		Mo*Kα* λ=0.71073 Å		
X-ray power		50 kV, 30 mA		
Monochromator		Graphite		
Temperature (°C)	25	150	350	25
Time per frame (s)	10	10	10	10
Max. 2θ	74.01	72.64	66.28	34.22
Index ranges	-23 < *h* < 22	-23 < *h* < 22	-19 < *h* < 20	-10 < *h* < 10
	-30 < k < 30	-30 < k < 30	-26 < k < 26	-13 < k < 13
	-29 < l < 30	-29 < l < 30	-24 < l < 24	-13 < l < 12
No. of measured reflections	32614	61087	51278	4504
No. of unique reflections	4600	9762	7336	1009
No. of observed reflections *I* > 2*σ (I)*	3651	6775	5721	820
Structure refinement				
No. of parameters used in the refinement	207	327	339	140+1
R(int)	0.0357	0.0487	0.0504	0.1481
R(σ)	0.0342	0.0336	0.0312	0.0919
GooF	1.086	1.010	1.042	1.313
*R*1, I>2*σ (I)*	0.0379	0.0414	0.0494	0.1181
*R*1, all data	0.0507	0.0701	0.0685	0.1383
w*R*2 (on F^2)	0.1193	0.1249	0.1334	0.3204
$\Delta\rho_{min}$ (-eÅ^{-3}) close to	-0.47 W1	-0.51 T1	-0.50 T5	-0.81 O1
$\Delta\rho_{max}$ (eÅ^{-3}) close to	0.76 W9	0.68 O7	0.70 O9	0.80 O15
BASF	0.364(4)	0.504(3)	0.431(3)	

Table 2b Crystal data and refinement parameters of Na-stilbite at RT, 150 (RH ~ 0) and, 350 (RH ~ 0).

Crystal data	**Na-stilbite1 A RT**	**Na-stilbite1 B 150°C**	**Na-stilbite1 B 350°C**
Crystal size (μm)	100 x 350 x 500	100 x 350 x 500	100 x 350 x 500
a-axis (Å)	13.6165(4)	13.6685(3)	13.6092(3)
b-axis (Å)	18.2201(5)	17.2388(4)	17.1490(3)
c-axis (Å)	17.8325(7)	16.7121(4)	15.9990(4)
β (°)	90.012(3)	90.019(2)	90.0120(10)
Cell volume (Å^3)	4424.1(2)	3937.85(16)	3733.9(14)
Z	1	1	1
Space group	*F*2/*m*	*A*2/*m*	*A*2/*m*
Refined chemical formula	$Na_{13.89}(Si,Al)_{72}O_{144}\cdot 56.3H_2O$	$Na_{13.98}(Si,Al)_{70.99}O_{144}\cdot 7.0H_2O$	$Na_{14.25}(Si,Al)_{72}O_{144.4}$
Data collection			
Diffractometer		Bruker APEX II SMART	
X-ray radiation		Mo$K\alpha$ λ=0.71073 Å	
X-ray power		50 kV, 30 mA	
Monochromator		Graphite	
Temperature (°C)	25	150	350
Time per frame (s)	10	10	40
Max. 2θ	74.07	64.06	65.00
Index ranges	-22 < *h* < 22	-20 < *h* < 20	-20 < *h* < 20
	-30 < k < 30	-25 < k < 25	-25 < k < 25
	-28 < l < 30	-24 < l < 22	-24 < l < 21
No. of measured reflections	27311	32749	30647
No. of unique reflections	5697	6995	6896
No. of observed reflections $I > 2\sigma(I)$	4035	4359	5036
Structure refinement			
No. of parameters used in the refinement	207	330	339
R(int)	0.0509	0.0667	0.0547
R(σ)	0.0412	0.0609	0.0388
GooF	1.055	1.037	1.032
*R*1, I>2σ *(I)*	0.0439	0.0505	0.0531
*R*1, all data	0.0692	0.0977	0.0807
w*R*2 (on F^2)	0.1362	0.1490	0.1433
$\Delta\rho_{min}$ (-eÅ^{-3}) close to	-0.54 W9	-0.56 Na4	-0.52 T1M
$\Delta\rho_{max}$ (eÅ^{-3}) close to	0.65 W9	0.64 CW3	0.52 T1
BASF	0.502(5)	0.497(4)	0.502(3)

Table 3 Correspondence between tetrahedral sites in orthorhombic (*Amma*) and monoclinic (*A*2/*m*) space group.

Orthorhombic *Amma*	Monoclinic *A*2/*m*
T1	T2/T1M
T1P	T1/T2M
T3	T3/T3M
T4	T4/T4M
T5	T5/T5M
O3P	O3M/O5M
OD	OD/ODM

Table 4 Unit-cell parameters of natural stilbite (two different specimen from the same locality) and Na-exchange stellerite obtained by XRPD and SCXRD at RT. Standard (*C*2/*m*) and non-standard settings (*F*2/*m*) are reported.

XRPD						
	Stilbite1		Stilbite2		Na-stellerite	
	*C*2/*m*	*F*2/*m*	*C*2/*m*	*F*2/*m*	*C*2/*m*	*F*2/*m*
a-axis (Å)	13.6084(9)	13.6084(9)	13.5863(8)	13.5866(8)	13.6280(8)	13.6273(7)
b-axis (Å)	18.2487(5)	18.2486(3)	18.2286(2)	18.22860(13)	18.1910(10)	18.1908(3)
c-axis (Å)	11.2048(7)	17.8455(5)	11.2549(8)	17.8213(4)	11.2100(6)	17.8235(8)
β (°)	127.222(4)	90.194(5)	127.657(5)	90.537(7)	127.344(4)	90.076(6)
Volume (Å^3)	2215.7(3)	4431.6(3)	2206.7(3)	4413.5(3)	2209.4(3)	4418.3(3)
R_{Bragg}	0.21	0.25	0.66	0.63	0.21	0.22
Rwp (%)	4.99	4.99	6.57	6.58	4.19	4.19
SCXRD						
a-axis (Å)	13.6044(2)	13.6044(2)	13.6174(6)	13.6174(6)	13.6195(2)	13.6195(2)
b-axis (Å)	18.2482(2)	18.2482(2)	18.2287(8)	18.2287(8)	18.1646(3)	18.1646(3)
c-axis (Å)	11.2103(2)	17.8291(4)	11.250(4)	17.8446(7)	11.2086(3)	17.8200(5)
β (°)	127.3250(10)	90.0320(10)	127.358(2)	90.016(2)	127.3520(10)	90.060(2)
Volume (Å^3)	2213.08(6)	4426.18(13)	2214.75(2)	4429.5(4)	2204.26(8)	4408.54(16)
Transformation matrix from *C*2/*m* to *F*2/*m*: [100 0-10 -10-2]						

Supplementary_tables

Click here to download Supplementary Material: Supplementary_tables.docx

Supplementary_figure

Click here to download Supplementary Material: Supplementary_figures.docx

Cif

Click here to download Supplementary Material: stellerite_RT.cif

Cif

Click here to download Supplementary Material: Stellerite_125.cif

Cif

Click here to download Supplementary Material: Stellerite_175.cif

Cif

Click here to download Supplementary Material: Stellerite_300.cif

Cif

Click here to download Supplementary Material: Stellerite_400.cif

Cif

Click here to download Supplementary Material: Stilbite_RT.cif

Cif

Click here to download Supplementary Material: Stilbite_125.cif

Cif

Click here to download Supplementary Material: Stilbite_350.cif

Cif

Click here to download Supplementary Material: Na-stellerite_RT.cif

Cif

Click here to download Supplementary Material: Na-stellerite_150.cif

Cif

Click here to download Supplementary Material: Na-stellerite_350.cif

Cif

Click here to download Supplementary Material: Na-stellerite_exsitu_525.cif

Cif

Click here to download Supplementary Material: NA-stilbite_RT.cif

Cif

Click here to download Supplementary Material: NA-stilbite_150.cif

Cif

Click here to download Supplementary Material: Na-stilbite_350.cif

Supplementary Material

Click here to download Supplementary Material: Supplementary_FigureS2.docx